

**REPORT DOCUMENTATION PAGE**

0131

hering  
tion of

Public reporting burden for this collection of information is estimated to average 1 hour per response, including and maintaining the data needed, and completing and reviewing the collection of information. Send comment information, including suggestions for reducing this burden, to Washington Headquarters Services, Directorate for Information Operations and Reports, 1215 Jefferson Davis Highway, Suite 1204, Arlington, VA 22202-4302, and to the Office of Management and Budget, Paperwork Reduction Project (0704-0188), Washington, DC 20503.

1. AGENCY USE ONLY (Leave blank)		2. REPORT DATE 22 April 1999	3. REPORT TYPE AND DATES COVERED Final Technical 1 Sep 98 thru 28 Feb 99	
4. TITLE AND SUBTITLE High-Performance Liquid Crystal Adhesives			5. FUNDING NUMBERS F49620-98-C-0054	
6. AUTHORS Dr. Patrick J. Hood				
7. PERFORMING ORGANIZATION NAME(S) AND ADDRESS(ES) Cornerstone Research Group, Inc. 2792 Indian Ripple Rd. Dayton, OH 45440			8. PERFORMING ORGANIZATION REPORT NUMBER	
9. SPONSORING/MONITORING AGENCY NAME(S) AND ADDRESS(ES) Air Force Office of Scientific Research 801 N. Randolph St., Suite 732 Arlington, VA 22203-1977			10. SPONSORING/MONITORING AGENCY REPORT NUMBER	
11. SUPPLEMENTARY NOTES			19990528 064	
12a. DISTRIBUTION/AVAILABILITY STATEMENT Distribution Statement A. Approved for public release; distribution is unlimited.			12b. DISTRIBUTION CODE	
13. ABSTRACT (Maximum 200 words) High-temperature, easy-to-process adhesives are needed for adhesively bonded joints, and composite patch repair. Resins, such as epoxies, that are currently used are processable at temperatures below 200°C but have low upper-use temperatures. High-performance polyimides can be used at temperatures exceeding 300°C, but must be processed above 300°C. Low processing temperatures are needed for easy field repair as well as cost effective manufacturing processes. It is most desirable to have materials that are both easy to process and have high thermal stability. A high-temperature, low-shrinkage, easy-to-process adhesive based on liquid crystal monomers with reactive end groups was developed and evaluated in this program. In addition, an integrated fiber sensor for sensing moisture in the adhesive was investigated. During the Phase I effort a high-performance liquid crystal monomer was synthesized and a fiber optic moisture sensor was demonstrated. The liquid crystal monomer was evaluated and showed thermal stability up to 300°C with curing below 150°C. A Phase II proposal has been submitted focusing on further development and characterization of the adhesive material.				
14. SUBJECT TERMS adhesive, liquid crystal, fiber optic sensor, thermoset, spectral monitor			15. NUMBER OF PAGES 25	
			16. PRICE CODE	
17. SECURITY CLASSIFICATION OF REPORT UNCLASSIFIED	18. SECURITY CLASSIFICATION OF THIS PAGE UNCLASSIFIED	19. SECURITY CLASSIFICATION OF ABSTRACT UNCLASSIFIED	20. LIMITATION OF ABSTRACT	

# High-Performance Liquid Crystal Adhesives

## Table of Contents

<i>Program Overview</i> _____	2
<i>Technical Objectives</i> _____	3
<i>Technical Results – LC Adhesive</i> _____	4
<b>Materials Development</b> _____	4
<b>Characterization of LC Monomer RM 257 (Monomer I)</b> _____	6
<b>Synthesis and Characterization of LC monomer JNM-1 (Monomer II)</b> _____	6
<b>Mechanical Characterization</b> _____	8
<b>Fracture Mechanics Toughness Tests</b> _____	10
<b>Adhesion Testing</b> _____	12
<b>Moisture Susceptibility</b> _____	12
<b>Related Work in Materials Development</b> _____	12
Liquid crystal thermosets and adhesives: _____	12
Adhesively Bonded Joints: _____	12
Cure shrinkage analysis: _____	13
Non-destructive evaluation (NDE) _____	13
LC and Thermostable Polymer Development _____	14
<i>Technical Results - Fiber Optic Moisture Sensor Development</i> _____	15
<b>Background</b> _____	15
<b>Experimental Results</b> _____	18
Sol-Gel Cladding _____	18
ESA Monolayers _____	19
Polymer / Indicator-Salt Solution Cladding _____	19
Sol-Gel Glass _____	19
Doped Ceramics _____	20
<i>Conclusions</i> _____	23
<i>References</i> _____	24

## Program Overview

High-temperature, easy-to-process adhesives are needed for adhesively bonded joints, and composite patch repair. Resins, such as epoxies, that are currently used are processable at temperatures below 200°C but have low upper-use temperatures. High-performance polyimides can be used at temperatures exceeding 300°C, but must be processed above 300°C. Low processing temperatures are needed for easy field repair as well as cost effective manufacturing processes. It is most desirable to have materials that are both easy to process and have high thermal stability. These resins must also be resistive to hydrothermal degradation, since moisture aging is common in most aircraft applications. In addition to having good thermal stability, patch adhesives need to be tough and resistant to fatigue crack growth.

Cornerstone Research Group, Inc. (CRG) and the University of Dayton Research Institute (UDRI) proposed to develop and evaluate high-temperature, low-shrinkage, easy-to-process adhesives based on liquid crystal monomers with reactive end groups. In addition, we proposed to design and develop an integrated fiber sensor for sensing moisture in the adhesive. Our ultimate objective was to integrate this adhesive with an aircraft patch system that includes an integrated sensor to monitor the chemical integrity of the adhesive with time (see Figure 1). The sensor would enable routine field inspections of patch "health" to identify pre-micro-crack degradation of the adhesive caused by chemical attack from moisture and/or oxidation.

Summarized results of the Phase I program are:

- Synthesized high performance liquid crystal monomer
- Demonstrated thermal stability up to 300°C
- Demonstrated sub-150°C curing of the liquid crystal adhesive
- Demonstrated a fiber optic humidity sensor
- Identified an adhesive patch / sensor package
- Identified near-term commercial outlets for both adhesive and sensor technologies

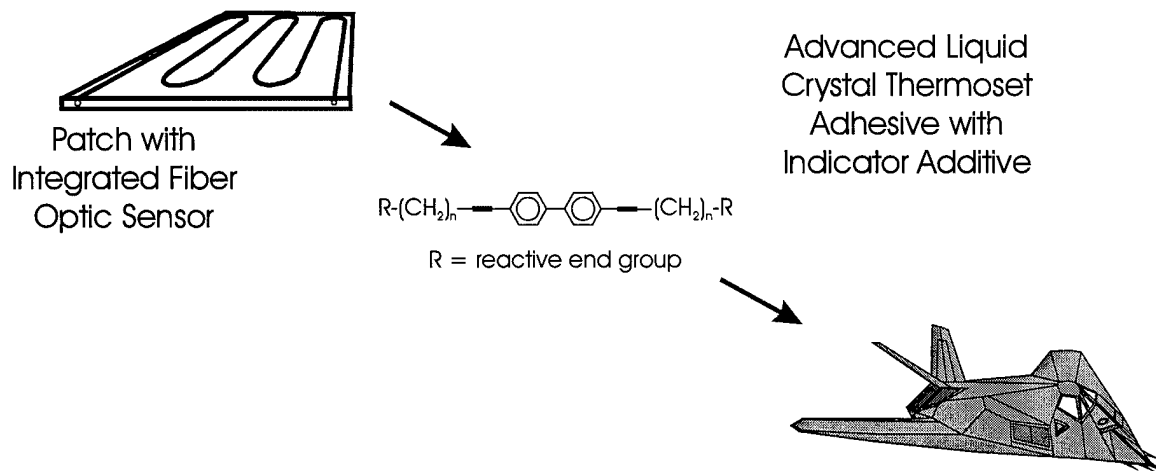


Figure 1: Program Overview

## Technical Objectives

The technical objectives of this program were to: 1) develop an easy-to-process, high-performance adhesive that has low moisture sensitivity and reduced cure shrinkage compared with conventional resins; and 2) develop specific fiber optic sensor approaches to detecting both hygrothermal and oxidative aging of adhesives. The specific technical objectives to be completed are given below.

- Show that the proposed monomer system can be processed at or below 150 °C to yield an adhesive that is thermally stable up to 300 °C.
- Evaluate catalyst systems for promoting cure of the reactive end groups at low (<100°C) temperatures to allow cure in the smectic LC phase.
- Show that to cure in the high-density smectic phase will result in reduced cure shrinkage.
- Establish that moisture sensitive coatings are available that are thermally stable at the expected use temperatures.
- Analyze thermal, thermal-oxidative and hygrothermal stability of at least one monomer in the series.
- Providing lap-shear (dry and wet) data for one monomer in the proposed series.

Fiber-optic sensor development work included analyzing sensor indicator materials for changes in visible light absorption after thermal/oxidative and hygrothermal aging. Specific technical objectives to be completed are given below.

- Compile a list of possible fiber optic coating materials for moisture analysis and thermal/oxidative degradation analysis.
- Measure the thermal stability of the proposed materials.
- Quantify the range of sensitivity of the proposed materials.

During the course of the Phase I effort the majority of these objectives were met. The following sections summarize the results from both the Materials Development Tasks and the Sensor Development tasks.

## Technical Results – LC Adhesive

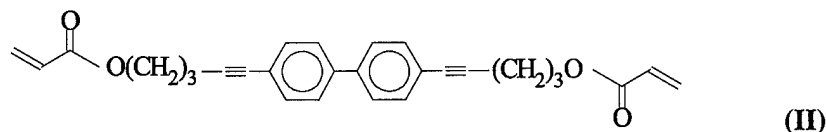
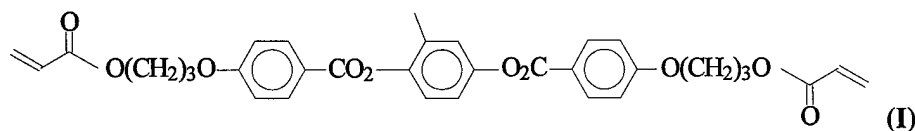
### Materials Development

There are many advantages to the proposed materials system over currently available materials.

- Curing temperature is below 150°C – suitable for field repair and/or cost effective manufacturing processes – with the cured material having a  $T_g$  above 300°C.
- E-Beam curing of joints at room temperature enables low-cost manufacturing processes with high-performance materials.
- Liquid crystal nature of polymer should provide high shear strength and toughness.
- Adhesive inherently has a low susceptibility to chemical attack by moisture.
- The bond is single component and can be melt processed eliminating the need for solvents during bonding.
- Adhesive would be formed into an uncured film eliminating the need for refrigeration of resins in the field.

The materials system is based on a monomer type that is dual curing and can be polymerized at relatively low temperatures to form adhesives thermally stable to 300°C. The proposed monomer series ( $n = 3, 5, 7$ ) can form liquid crystal (LC) phases. For example, when  $n = 3$ , a smectic LC phase exists above room temperature. Because the LC phase allows tight packing of molecules it has a higher density than the isotropic phase. Cure in the smectic phase should result in lower overall cure shrinkage than typical isotropic monomers exhibit. Lower thermal expansion coefficients can also result from cure of a LC material.

The approach followed in the Phase I program was to demonstrate the feasibility of using single component thermotropic liquid crystal (LC), addition curing monomers to form adhesives that both cure at low temperatures and achieve high glass transition temperatures. The emphasis in these studies was on thermal curing systems. For demonstrating the proof of concept, two LC monomers were studied, a nematic LC diacrylate **I** and a smectic LC dual functional monomer **II** [shown below].



The monomers have LC phases as shown in the DSC scans of Figures 2 and 3, respectively.

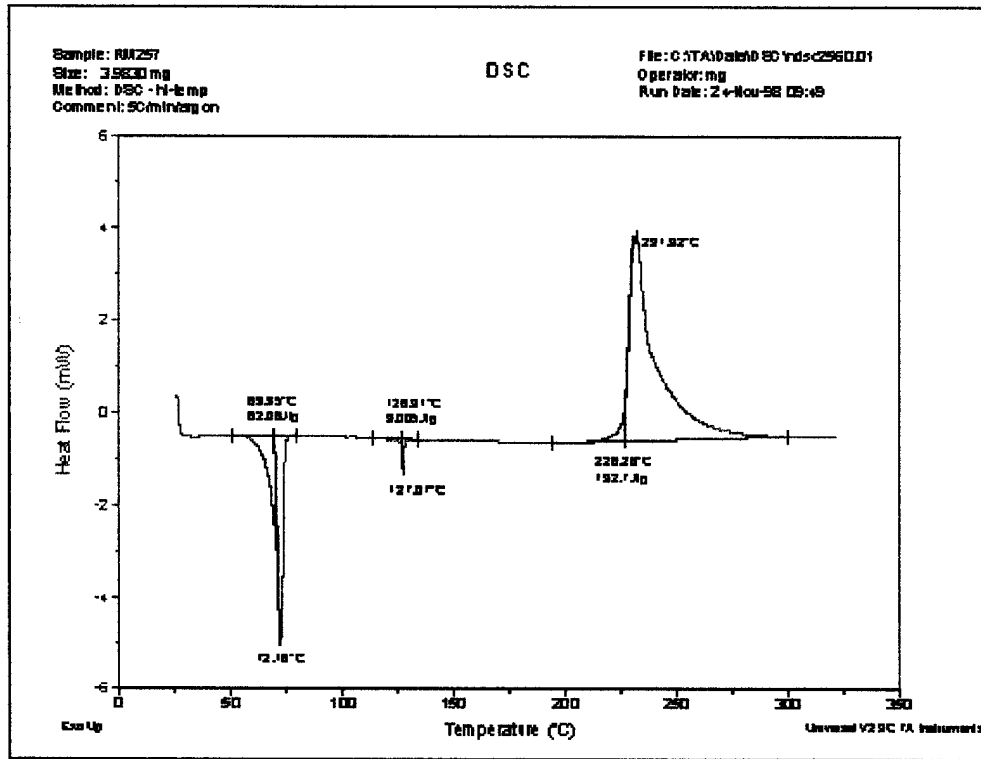


Figure 2: DSC of Monomer I

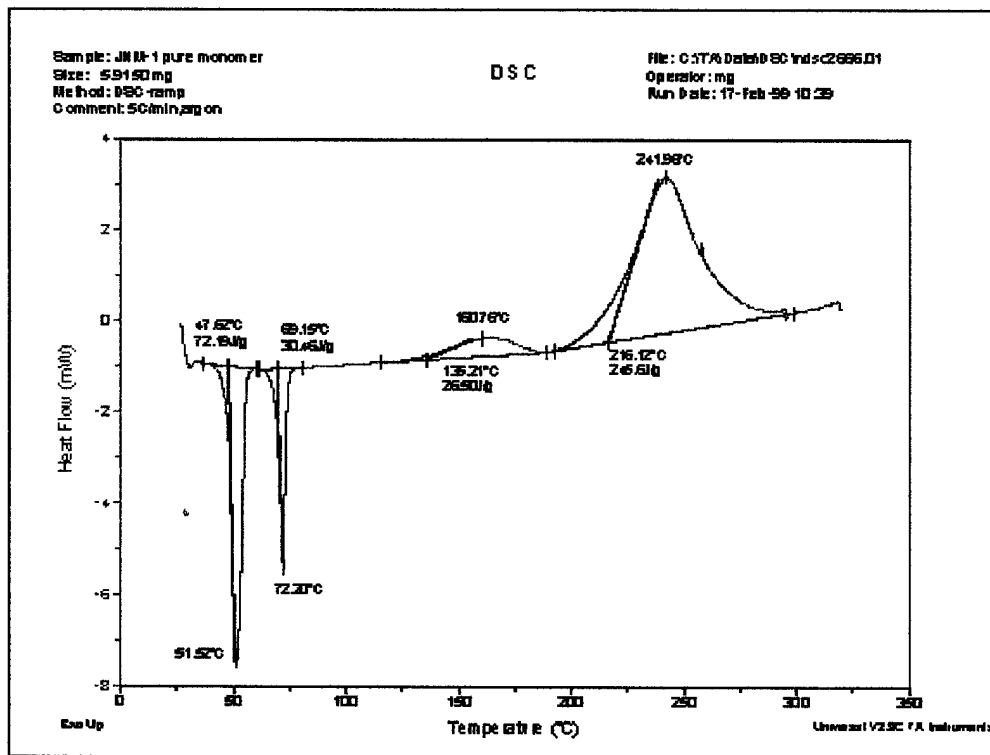
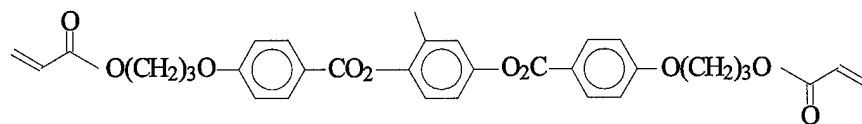


Figure 3: DSC of Monomer II

The initial research on these monomers involved photocuring using UV radiation<sup>1,2</sup>. The monomers also can be cured thermally. Determining the salient features of thermal curing for adhesive processing was a principal part of the Phase I research program. In summary the results are as follows:

### **Characterization of LC Monomer RM 257 (Monomer I)**

1. RM 257 is an acrylate terminated mesogen which has a nematic LC phase above the crystalline melting point,  $T_m = 69^\circ\text{C}$ ; the nematic to isotropic clearing temperature is  $127^\circ\text{C}$  (see Figure 1). Thermal cure of the pure monomer occurs at high temperatures in the range of  $230\text{-}250^\circ\text{C}$ .

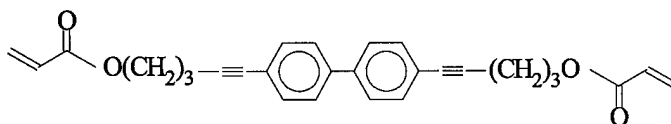


RM257 was compounded with benzoyl peroxide, a common thermal initiator, at different concentrations. DSC data on the thermal polymerization of RM257 with benzoyl peroxide were collected. The data showed the following:

1. The thermal polymerization is effectively initiated by the peroxide, with reaction occurring in the temperature range of the thermal decomposition of the peroxide (starting at  $110^\circ\text{C}$ ).
2. As the peroxide concentration increases the percent conversion of monomer at low temperatures increases.
3. Residual reaction of remaining unreacted acrylate groups occurs at higher temperatures; however, the high temperature reaction exotherm shifts to lower temperatures as peroxide concentration increases.
4. The reaction initiates in the nematic liquid crystal phase.
5. The experiments prove the viability for thermal initiation in the LC phase.
6. The LC phase morphology is "locked-in" by crosslinking
7. We also considered the lower temperature initiators AIBN and lauryl peroxide. AIBN only slightly reduces the cure temperature but increases the % conversion obtained at temperatures in the range of  $110\text{-}120^\circ\text{C}$ . Lauryl peroxide did not perform as well as AIBN.
8. There are instability and shelf life issues to be considered when implementing low temperature thermal initiators: to be considered are use of an inhibitor and storage in the crystalline state as effective methods for insuring shelf life. Stabilization is one of the subjects for study in the Phase II program.

### **Synthesis and Characterization of LC monomer JNM-1 (Monomer II)**

1. JNM-1 is a dual functional monomer containing both acrylate and acetylene reactive groups. It has a smectic LC phase above the crystalline melting point,  $T_m = 50^\circ\text{C}$ . The smectic to isotropic transition is  $71^\circ\text{C}$  (see Figure 2).



(a) JNM-1 was successfully synthesized. The purity of the monomer is  $> 98\%$  as determined by HPLC. Characterization of the JNM-1 monomer shows the following:

- (a) JNM-1 was successfully synthesized. The purity of the monomer is > 98% as determined by HPLC. Characterization of the JNM-1 monomer shows the following:
  - (b) H NMR and FTIR spectra of the monomer are consistent with the chemical structure cited above.
  - (c) Transition temperatures for the synthesized LC monomer (obtained by DSC) are consistent with the values cited above.
  - (d) The LC phase above 50°C is tentatively assigned as a smectic LC phase.
  - (e) On cooling from the isotropic phase the monomer goes into the smectic phase at  $T_m$  and supercools with crystallization occurring at around 10°C.
  - (f) The monomer containing benzoyl peroxide polymerizes in the isotropic state around 123°C.
  - (g) AIBN is also an effective thermal initiator for Monomer II. AIBN slightly reduces the cure temperature to around 110°C; it also increases the % conversion obtained at temperatures in the range of 110- 120°C. The data shown in Figure 4 indicate that the initial % conversion of monomer obtained at low temperatures increases at AIBN concentrations up to 0.75% by weight.
2. Thermal-gravimetric analysis data, shown in Figure 5, show that the thermal-oxidative stability of polymerized Monomer II, as measured by weight loss, extends to well above 300°C.

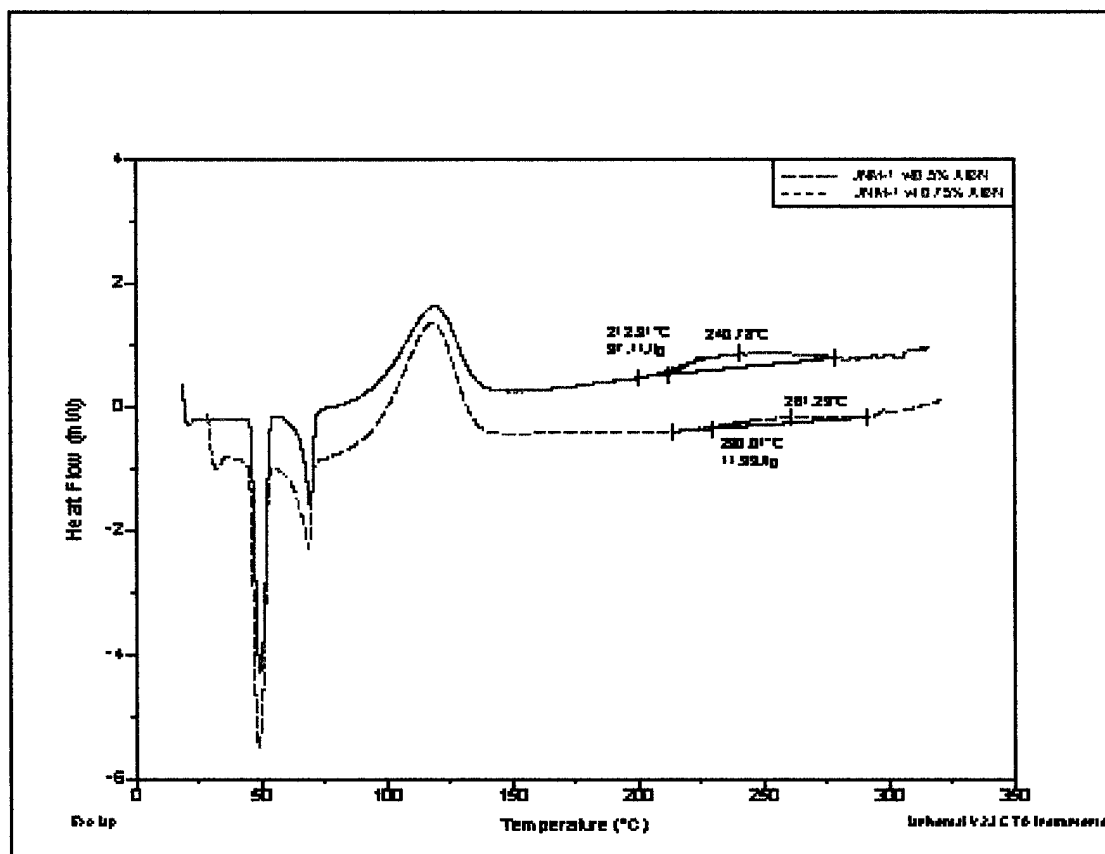


**Figure 4: DSC of Monomer II (JNM-1) with AIBN**

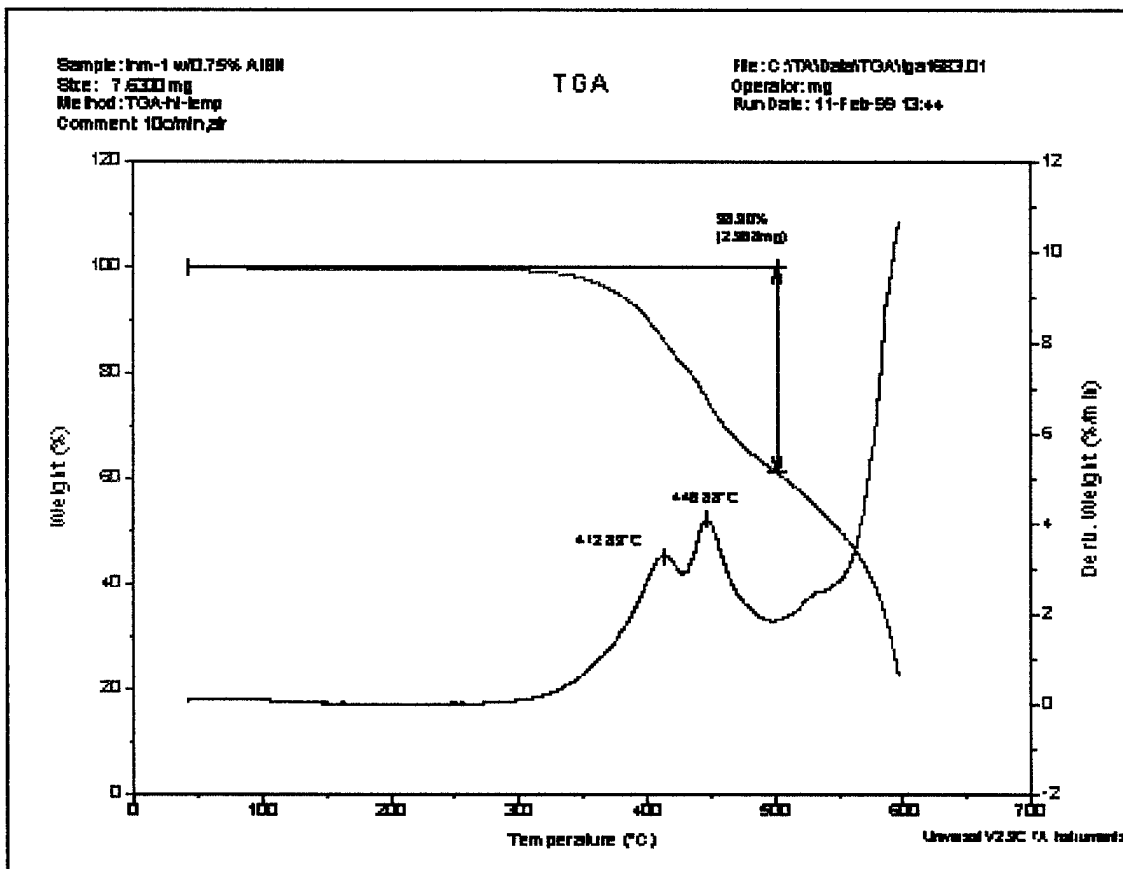


Figure 5: Thermal-Gravimetric Analysis of Monomer II (JNM-1) with AIBN

### Mechanical Characterization

Dynamic mechanical analysis (DMA) results confirm that the LC monomers considered can be cured to form crosslinked polymers with high glass transition temperatures. Monomer I, which has a modest ultimate  $T_g$  of 150°C, still has a rather high modulus above  $T_g$  as shown in Figure 6. In Figure 6 the storage moduli of photocured Monomer I and a similar ester LC monomer are compared with moduli values of two low temperature curing epoxies. Photocuring of Monomer II in both LC and isotropic phases results in polymers with high  $T_g$  values in excess of 300°C as shown in Figure 7. These results were obtained in a previous program where it was shown that crosslinking can be accomplished by photo-reaction. It is clear that the LC monomers have both higher  $T_g$  values and retain greater modulus values above  $T_g$ . This is highly relevant to the Phase II program because low temperature e-beam curing is proposed. The same monomers that perform well in the photocuring mode also should perform well in the e-beam cure mode.

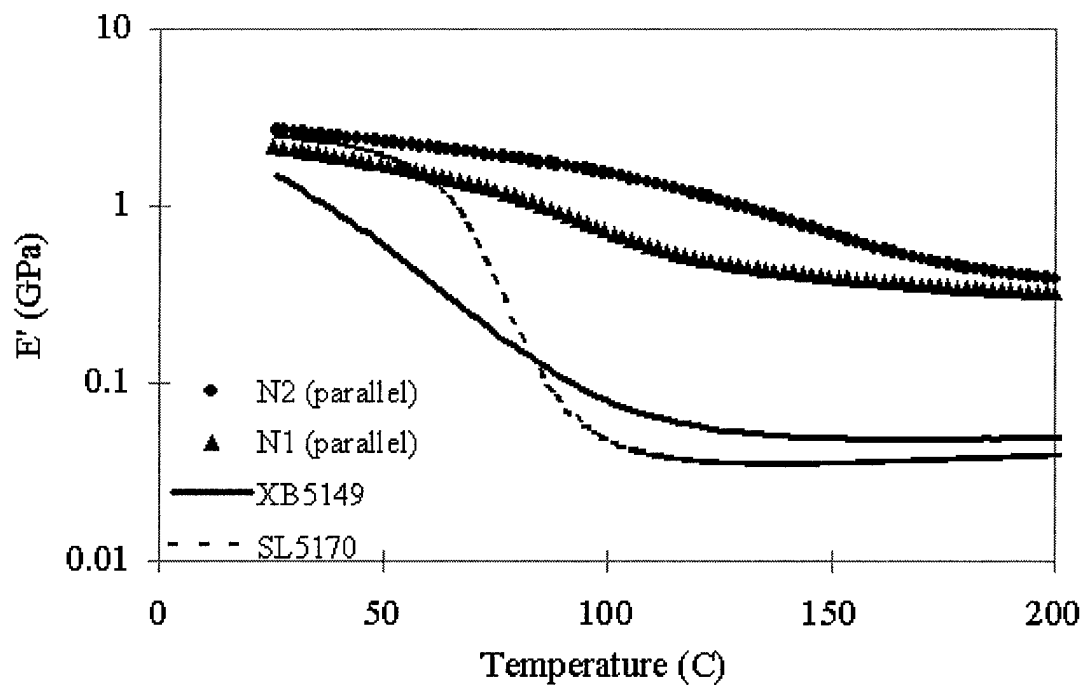


Figure 6: DMA of Photocured Monomer I.

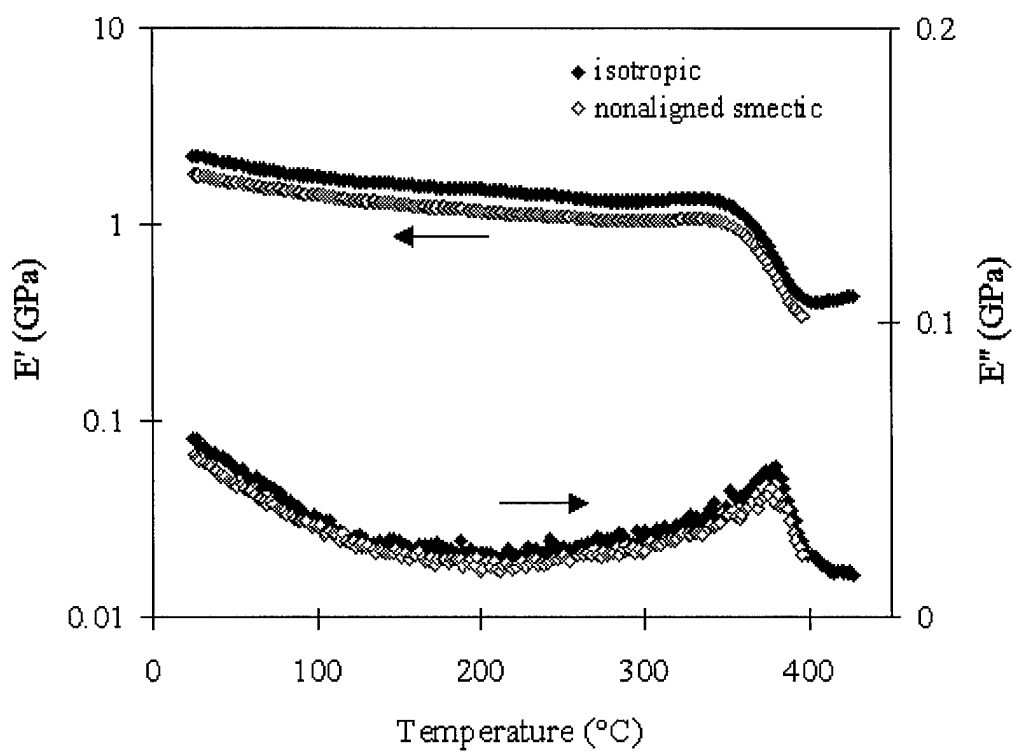


Figure 7: DMA Comparisons of Photocured Monomer II

In the Phase I AFOSR STTR program the cure mechanism was extended to thermal curing using free radical initiation as noted above. The data of Figure 8 indicate that the dual curing Monomer II can be thermally cured to attain exceptionally high  $T_g$  values, provided that a suitable high temperature post-cure is employed. The need for high temperature post-cure is reduced as the initiator concentration is increased. One of the goals of the Phase II program will be to further reduce the temperature of cure by optimizing the type and concentration of thermal initiator and by considering low temperature e-beam curing.

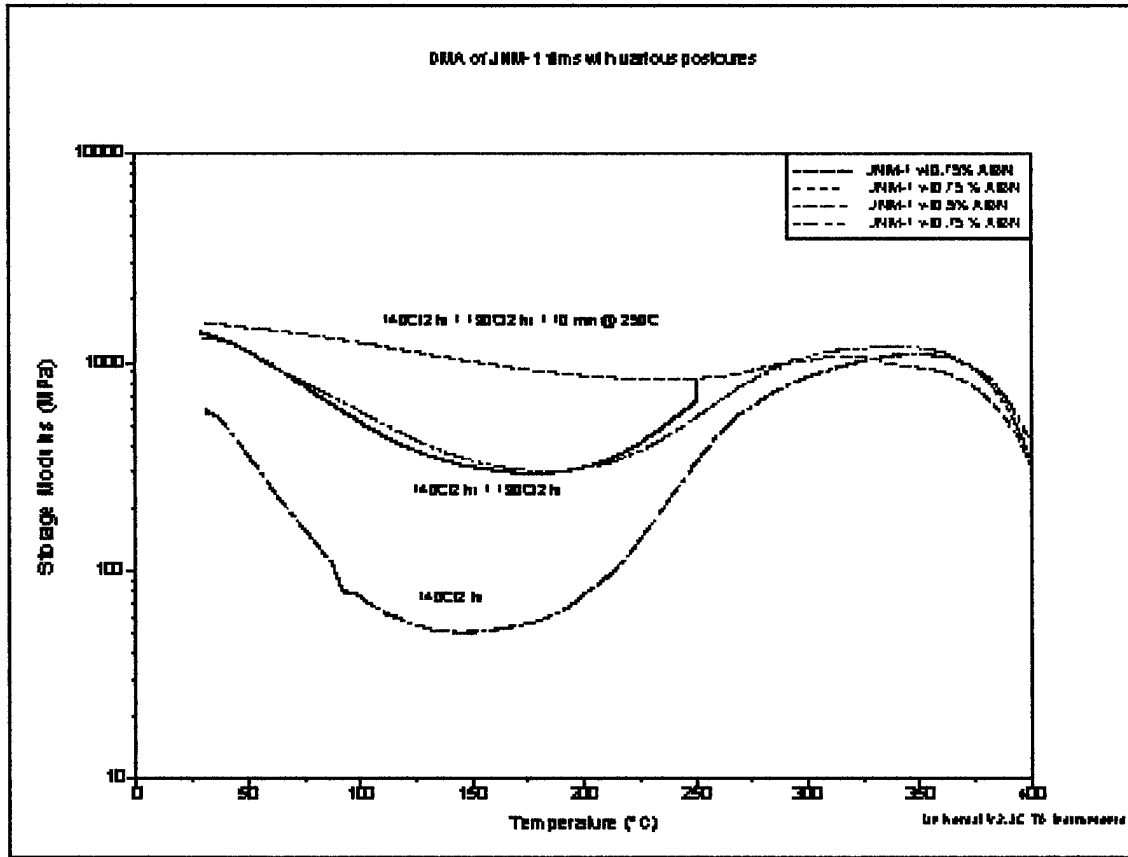


Figure 8: DMA of Monomer II Films with Various Postcures

### Fracture Mechanics Toughness Tests

Room temperature fracture mechanics analysis for toughness was carried out for Monomer I, which was photocured<sup>3</sup>. Miniature compact tension specimens were prepared from samples cured in both the LC state and the isotropic state. Stress analysis of crack propagation in a brittle material leads to the concept of a stress intensity factor,  $K$ , which describes the stress field surrounding the crack tip.  $K_Q$  is the value of the stress intensity factor where a material begins to crack significantly. Mean  $K_Q$  values were: for nematic  $K_Q = 290 \text{ psi}\sqrt{\text{in}}$  (std. dev. 31%), and for isotropic  $K_Q = 639 \text{ psi}\sqrt{\text{in}}$  (std. dev. 12.7%).

The substantial difference in toughness in these materials are attributed to the differences in morphology of the material cured in the two different physical states. Figure 9 is the polarized photomicrograph of Monomer II after photopolymerization in the smectic phase. Note the areas of localized order, which adds to the toughness of the matrix. The samples cured in the isotropic state, as shown in Figure 10a, had very smooth fracture surfaces resulting in fast, low energy crack propagation. The samples cured in the LC state, as shown in Figure 10b, retained the characteristic smectic domain "morphology" which resulted in considerable crack deflection and higher stress intensities for fracture.

Both materials were post-cured under the same conditions. Thus, one objective for the Phase II program is to exploit the potential advantage obtained by curing in the LC state to lock in the LC morphology in order to achieve enhanced toughness.

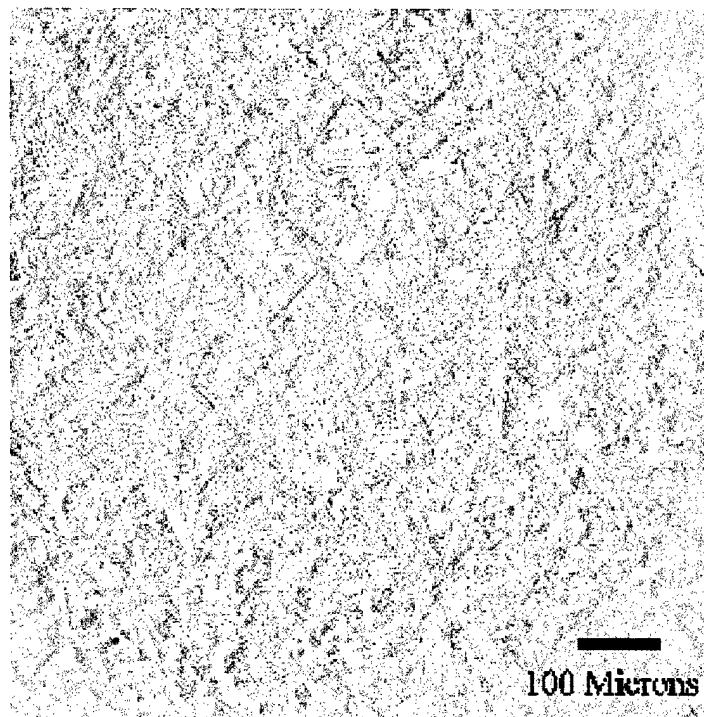


**Figure 9: Polarized photomicrograph of Monomer II after photopolymerization<sup>4</sup>**

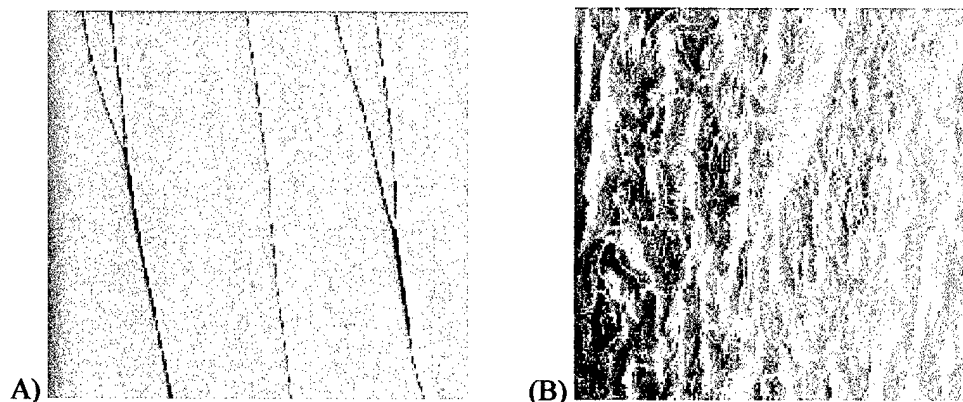


**Figure 10: Isotropic (A) and Smectic (B) Phase Fracture Surfaces of Monomer II**

### ***Adhesion Testing***

Preliminary lap-shear adhesion tests were carried out on four samples following the standard ASTM D1002 procedure. The aluminum adherend surfaces were grit blasted and a primer was applied but no attempt was made to optimize the surface preparation or primer system. The maximum shear strength

### ***Adhesion Testing***

Preliminary lap-shear adhesion tests were carried out on four samples following the standard ASTM D1002 procedure. The aluminum adherend surfaces were grit blasted and a primer was applied but no attempt was made to optimize the surface preparation or primer system. The maximum shear strength obtained for thermally cured Monomer II was 1370 psi. While this value is low, failure was clearly adhesive with clean debonding from one of the adherends observed in all cases. Thus in the Phase II program efforts will be directed toward optimizing surface preparation for wetting and bonding by matching polymer and adherend surface energies and acid base characteristics. The emphasis will be on obtaining excellent interfacial characteristics to maximize adhesive strength.

### ***Moisture Susceptibility***

Preliminary humidity exposure data on a fully cured sample of Monomer II indicates excellent moisture retention characteristics. The sample, aged in 95 % RH air at 71°C for 1 week, picked up 1.65% moisture. This is much lower moisture retention than most epoxy adhesives. Of interest in the Phase II program will be characterizing the effects of hot, wet conditions on the  $T_g$ , mechanical properties, and adhesive bond strength in the LC materials.

### ***Related Work in Materials Development***

#### ***Liquid crystal thermosets and adhesives:***

Although liquid crystal thermosets have not been widely studied, there is some reference to adhesive applications in the literature. Frich and Economy<sup>4</sup> studied liquid crystal aromatic copolyesters as adhesives for titanium. Excellent bonding to titanium was achieved. The materials exhibited high thermal stability, low moisture pick-up, and lower thermal expansion compared with non-LC analogue monomers. Ober and Barclay<sup>5</sup> report on the use of LC thermosets based on triazine and epoxy networks for micro-electronics packaging. They found that the networks with the highest crosslink density resulted in the lowest CTE values. CTE values as low as 15 ppm/°C were achieved with aligned specimens. Jones, Jr. et al.<sup>6</sup> of the Dow Chemical Co. have a patent (United States 5,248,360) describing the preparation of carbon fiber reinforced composites having thermosetting liquid crystal matrices. They found that the composites made with LC monomers to have improved mechanical properties.

The University of Dayton has developed LC resins for use in stereolithography and other applications<sup>7-17</sup>. Under NSF Grant # DMR-9420357, LC resins having upper use temperatures in the range of 150 to 300°C were synthesized. A modified stereolithography process was developed to allow layer-by-layer alignment of the LC resin. It was found that part properties, such as thermal expansion coefficients, could be predicted using laminate theory. Room temperature CTE values as low as 12 ppm/°C were measured for aligned multi-layer parts.

#### ***Adhesively Bonded Joints:***

The Adhesives and Composites Group (ACG) at The University of Dayton has been conducting research projects related to the processing and characterization of polymeric composite materials and adhesively bonded joints for 40 years. Customers have included all branches of the DoD, NASA, and many industrial organizations in the aerospace, automotive, medical, construction and materials supplier fields.

The ACG has been a leading source of mechanical and environmental property data for advanced composite materials, adhesives, environmentally compliant bonding primers, and aluminum surface preparations for bonding. High temperature (service temperature over 260°C) adhesives have been extensively evaluated. Many types of adhesives have been evaluated to determine suitability for on-

aircraft bonded repair in the field. Several novel processes for repairing damaged metallic structure with bonded composite material patches were developed in the ACG. Some of these procedures are being widely adopted in both the military and commercial sectors for repair of aging aircraft. Improved test methods for evaluating adhesive properties were developed by the ACG. Personnel from the ACG have headed task groups within ASTM that developed new standards and specifications for adhesive materials, bonding primers, and bonding procedures. A variety of equipment for implementing adhesive bonding in on-aircraft field repair scenarios has been conceived, designed, constructed, and demonstrated for the Air Force. These items are currently being used by numerous AF organizations to carry out adhesive bonded structural repair of damaged aircraft.

The ACG possesses a wide array of equipment for processing and testing composite and adhesive materials and an extensive capability to subject these materials to various environmental exposure conditions to determine their durability under harsh to extreme conditions.

### *Cure shrinkage analysis:*

Traditional thermosetting resins experience volumetric cure shrinkage on the order of 7 to 20 %. Three factors contribute to volumetric shrinkage: the formation of covalent bonds, decrease in packing density, and thermal expansion resulting from cooling to ambient temperature from the cure temperature. If the material is restricted from shrinking, residual stresses occur that may lower the ultimate strength of the material. To reduce cure shrinkage, one or more of the three contributing factors must be addressed.

In the monomer, molecules are located at a van der Waals' distance from each other. In the corresponding polymer, the molecules are a covalent distance apart. In a condensation reaction, a small molecule is eliminated during the formation of a bond between molecules resulting in shrinkage. The amount of shrinkage is a function of the size of the molecule eliminated. During addition polymerization no small molecule is eliminated, however, significant shrinkage still results from the closer proximity of atoms in the polymer compared to the monomer. In ring-opening polymerization, the shrinkage may be less than in either case above. In this type of reaction, for every bond that undergoes a change in van der Waals' distance to a covalent bond, another bond goes from a covalent distance to a van der Waals' distance. Then, shrinkage is related to the number of rings being opened per unit volume as well as the size of the rings. With some bicyclic monomers volumetric expansion can result from polymerization<sup>18</sup>.

Another approach to reducing cure shrinkage is to polymerize from a high density phase. For example, going from a crystalline monomer to an amorphous or less-ordered semi-crystalline polymer may result in reduced shrinkage. A monomer cured in a smectic liquid crystal phase starts with a much higher packing density than an amorphous monomer.

The Center for Basic and Applied Polymer Research at the University of Dayton has considerable experience in measuring cure shrinkage and has developed novel techniques for measuring the real-time shrinkage of ultra-fast curing photo-monomers<sup>17,19,20</sup>. Projects involving shrinkage analysis have been sponsored by Sandia National Laboratories<sup>19</sup>, EMTEC<sup>20</sup>, and the National Science Foundation<sup>17</sup>. In recent work sponsored by the NSF, an optical technique was developed to measure the linear shrinkage of nematic liquid crystal monomers cured by a UV laser. The Polymer Center also has expertise in applying conventional thermal-dilatometry techniques to analyzing cure shrinkage resulting from chemical reaction and thermal contraction.

### *Non-destructive evaluation (NDE)*

NDE methods applicable to adhesive-bonded composite joints include ultrasonics, acoustic emission, radiography, holography, and thermography. Each method has its strengths and weaknesses. All of the methods can detect disbonds but none of them are capable of measuring small chemical changes in the adhesive that may result in loss of strength. Environmental aging can strongly influence bond strength and integrity. Davis et al.<sup>21</sup> of Lockheed Martin showed that substantial hydration is responsible for

bond failure in aluminum joints. They proposed a method based on electrochemical impedance spectroscopy to measure moisture absorption in adhesive bonds. As part of a recent project sponsored by the Air Force (Air Force Contract F33615-95-D-5616), the University of Dayton researchers used simple resistivity measurements to follow moisture absorption of an adhesive.

#### *LC and Thermostable Polymer Development*

The University of Dayton has been involved in research and development on thermostable polymers for adhesives and composites for many years. These programs have included synthesis, characterization, and mechanical property evaluations as well as field application studies. Much of this work has been done under the sponsorship of the WPAFB, USAF. Previous programs have included synthesis and characterization of specialty monomers and polymers such as various aromatic-heterocyclic polymers, acetylene terminated resins, PMR-polyimides, AFR-700 polyimides, PBO and PBT polymers.

The most recent work on functional LC monomers and polymers has concerned both structural and non-linear optical applications. In an NSF sponsored program several LC monomers containing both acrylate and acetylene functionality were developed that exhibited a desirable combination of properties including rapid cure at moderate temperatures, high  $T_g$  values, dual cure capability, and low moisture susceptibility. In related work the University has teamed with an industrial partner on development of similar LC monomers containing polar functions in their mesogenic cores for non-linear optical applications in waveguides and other electro-optical devices. A phase I SBIR program sponsored by the Air Force was completed recently and a phase II SBIR program began in April, 1998.

## Technical Results - Fiber Optic Moisture Sensor Development

### Background

Oxidation and corrosion lead to adhesion degradation and delamination. Water is a key offender in both mechanisms. We proposed to design and develop an integrated fiber sensor to sense water in the adhesive. The integrated fiber sensor would enable routine field inspection of patch "health" by identifying pre-micro-crack degradation of the adhesive caused by chemical attack from moisture and/or oxidation. The constraints of the sensor are as follows:

- Cannot affect integrity of the adhesive
- Embedded in adhesive
- No metal for LO aircraft
- Connector independent
- Low-cost
- Field-portable readout

Integrated optical sensors are typically sensitive, precise, embeddable, lightweight, and low-cost. They have three essential elements: the waveguide core, the waveguide cladding, and the sensing medium. In passive integrated optical devices, light is launched into the sensor, and follows the waveguide. The waveguide core guides the light through the device. The waveguide cladding confines the light in the core. In fiber optics, the waveguide core and the cladding are part of the fiber itself. The sensing medium is an indicator that changes spectral absorption properties with changing humidity. Coupling the waveguide to the necessary electronics can monitor these changes.

Over the past two decades, various types of fiber optic humidity sensors have been developed. Generally, they fall into one of the following four modes of sensors: transmission, porous fiber sensors, tip-coated (reflection) sensors, and side-coated (evanescent) sensors.<sup>22</sup>

In a transmission-mode sensor, the waveguide launches light into the sensing media. The light is then collected by a second waveguide, as depicted in Figure 11.

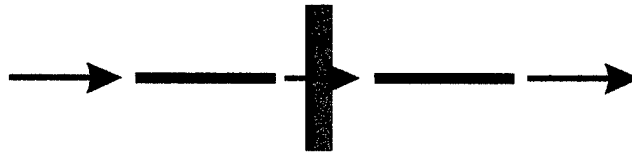
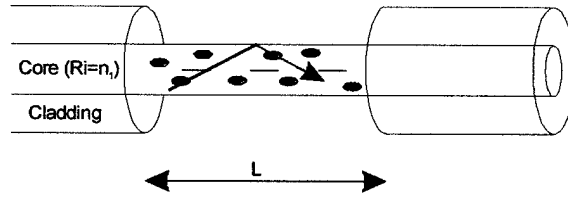


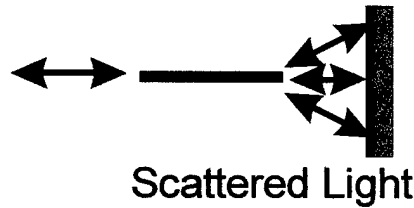
Figure 11: Transmission-mode Sensor

Figure 12 shows a porous fiber sensor, which is made by altering the fiber core. In this mode of sensors, light propagates through altered fiber core doped with water indicator. Zhou *et al.* began with a fiber of alkali borosilicate glass, a small section of which was heat treated to cause phase separation, resulting in a silica rich phase and an alkali borate rich phase.<sup>23</sup> The latter was leached away, leaving only a porous silica core. The sensor is created by immersing the treated portion of the fiber in a solution containing an indicator.



**Figure 12: Porous Core-mode Sensor**

In a reflective sensor, as depicted in Figure 13, the fiber launches light onto a reflective or scattering sensing media. Retroreflected light is collected by the same or an adjacent fiber. Reflection sensors are constructed either by coating the tip of the fiber with a cladding and indicator, then attaching a reflective film; or by coating a reflective surface with the indicator, then affixing the surface to the fiber end. The device may consist of either a bifurcated fiber, or a single fiber with a beam splitter, which separates the transmitted and detected rays.



**Figure 13: Reflective-mode Sensor**

The phenomenon of evanescence has frequently been used to create sensors. In an evanescent sensor, shown in Figure 14, light which is propagated down the waveguide is lost to the environment which is being sensed. The loss occurs over a length of the fiber that has a special cladding doped with an indicator. The cladding has a higher index of refraction than the fiber core, which causes the cladding to become the waveguide over the particular length of fiber. The light interacts with the indicator in the sensing medium, and as moisture is absorbed, the optical properties of the indicator change, changing the absorption of the spectrum.

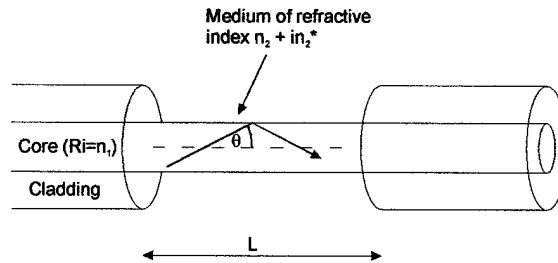


**FIGURE 14: Evanescent-mode Sensor**

The sensing media has two principle requirements. First, the sensing media must have an index of refraction greater than that of the core. Second, the absorption of the fiber must change as a function of the concentration of the conditions that are being monitored (i.e. moisture and oxidation.) It has been reported that the absorbance of such a sensor has either a linearly dependence on absorbance,  $\alpha L$ , or a nonlinear dependence taking the form of  $A=(\text{constant})(\alpha L)^n$  where  $n$  is less than unity depending on the optical design of the system and  $\alpha$  is the absorption coefficient ( $\alpha = 4\pi n_2^* / \lambda$ )<sup>24</sup>.

color change is directly proportional to the availability of water in the atmosphere and is completely reversible. The absorbance spectra of two different hydrochromic salts,  $\text{CoCl}_2$  and  $\text{CuCl}_2$  are shown in Figures 15 and 16, respectively. The “dry” spectra were acquired by dissolving the salt in water, and the “wet” spectra were acquired by adding water to the ethanol-salt solution.

As shown in Figures 15 and 16, a dramatic change in transmission occurs when the salt comes into contact with water. For the fiber optic sensor to detect these changes, it is necessary to measure the signal transmitted through the fiber sensor at at least two different wavelengths. One wavelength is selected at a point where a change in humidity generates a large change in absorption and the other wavelength is selected at a wavelength where little to no change in absorption takes place. In this way a ratio of the two signals can be used rather than an absolute power measurement. These characteristic wavelengths for  $\text{CoCl}_2$  are approximately 565-nm and 690-nm, respectively. For  $\text{CuCl}_2$ , the wavelengths are 605-nm and 425-nm, respectively.

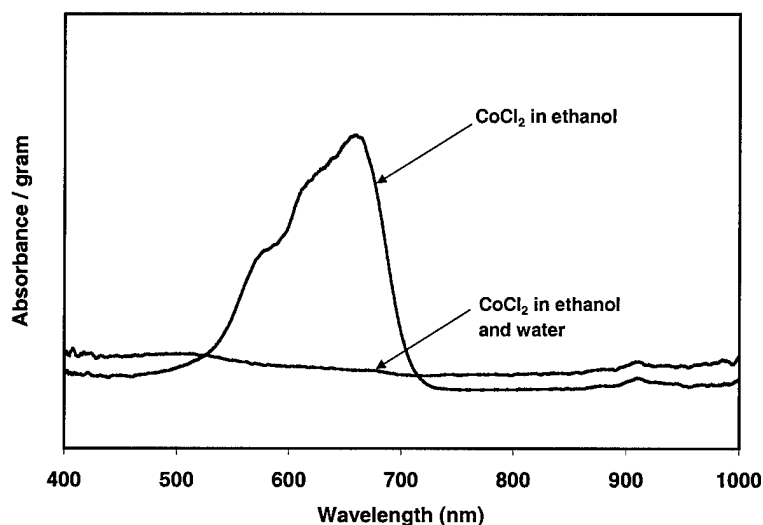


Figure 15: Hydrochromatic Salt:  $\text{CoCl}_2$

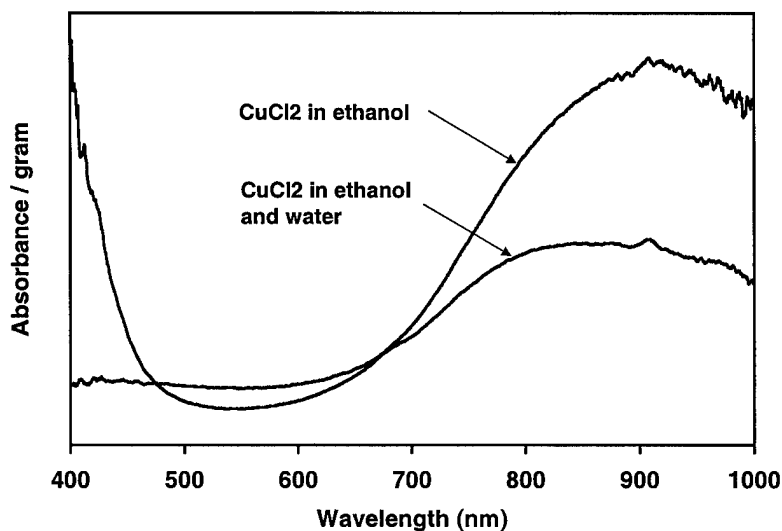


Figure 16: Hydrochromatic Salt:  $\text{CuCl}_2$

Modifying the concentration of the indicator in the sensing medium can alter the sensitivity of the device. A high concentration will have more drastic changes in the intensity of the light reflected when a large amount of moisture is absorbed, but very little change with small differences in humidity. When it is necessary to have high sensitivity, for example, 0% - 10% RH, the concentration of the indicator in the medium will be relatively low, as shown in Figure 17. If an application requires higher sensitivity in the upper regime, the concentration will be much greater. A wide range detector device can be fabricated by grading the concentration of the sensing material along the line length of the device.

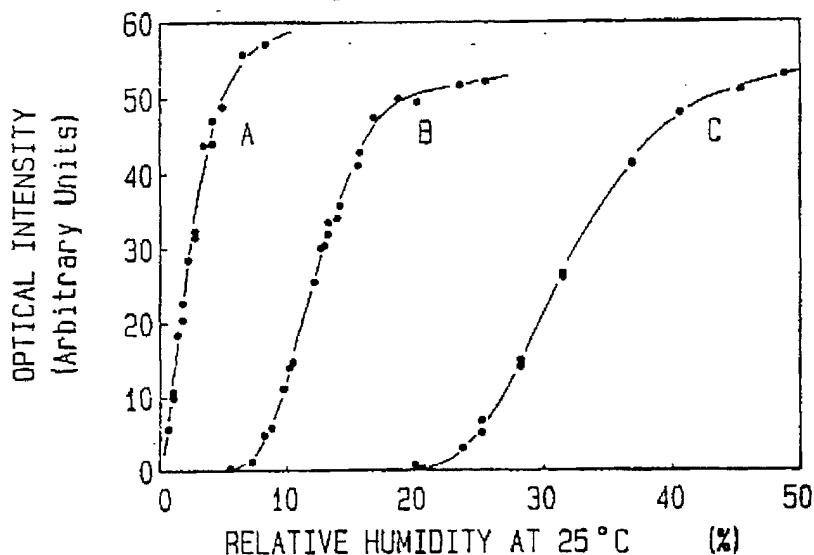


Figure 17: Relative Humidity Measurements for  $\text{CoCl}_2$  Concentrations: (A) 10 mg/ml; (B) 139 mg/ml; (C) 213 mg/ml<sup>23</sup>

### Experimental Results

CRG fabricated evanescent mode and reflective mode sensors. CRG did not fabricate transmission mode sensors because they do not demonstrate high precision accuracy due to loss and scatter. CRG also did not attempt to fabricate a porous fiber sensor. It is very expensive to have these specially fibers drawn, and capital costs are high to set-up a facility to fabricate them.

Our first attempts were at fabricating evanescent-mode sensors. For this type of sensor, it is necessary to suspend the indicator in another substance that will adhere to the waveguide. Three techniques that CRG utilized to create evanescent mode fiber sensors were sol-gel cladding, Electrostatic Self-Assembly (ESA) monolayers, and polymer / indicator-salt solution cladding.

#### Sol-Gel Cladding

In the sol-gel process, the precursor undergoes hydrolysis and polycondensation, forming a network of  $\text{SiO}_2$  bonds. Colloidal particles result when an adequate number of these bonds have formed; this mixture is termed a sol. CRG doped the sol with  $\text{CoCl}_2$ .<sup>25</sup> After a period of time, gelation, which is a dramatic increase in the viscosity of the fluid, occurred, and the sol became the gel. Glass slides were dipped, and fibers were drawn through the sol during gelation. Syneresis, or aging, required the gel to be immersed completely in water, continuing the hydrolysis and polycondensation. Aging increased the strength of the  $\text{SiO}_2$  bonds, and prepared the gel for drying.

The sol-gel films on glass slides were very brittle. We concluded that the fragile films were due to weak SiO<sub>2</sub> bonds, which were caused by poorly defined processing parameters. Because the strength of the SiO<sub>2</sub> bonds is directly related to the hydrolysis and drying times, these critical parameters must be optimized to achieve good quality films. The value of these parameters varied greatly in the literature: drying times varied from two weeks to two years. The optimization of these parameters based on these timetables would have been difficult to achieve in Phase I effort. Therefore we were unsuccessful in fabricating sol-gel-clad fibers.

### *ESA Monolayers*

Electrostatic self-assembly (ESA) bilayers were created by coating the fiber with alternating positively and negatively charged layers.<sup>26</sup> These bilayer deposits were created by alternating poly(allylamine hydrochloride) (PAH) and poly(sodium-4styrenesulfonate) (PSS). The final layer of PSS caused the surface to be negatively charge. The following set of bilayers was created by deposition of monolayers of ZrO<sub>2</sub> and a substance containing dissolved CoCl<sub>2</sub>.

Both PSS and ethanol were used as the second layer in the bilayer. The number of bilayers was varied to observe overall film thickness and optical properties. Samples were then cured at various temperatures and conditions.

The ESA films deposited on glass slides produced a moisture-sensitive cladding, but the films were very thin and hazy, which is indicative of scattering and signal loss. The processing of these films required large quantities of time, with poor quality of the yield. The glass substrates were found to soften beyond use at 600°C. Therefore, samples could not be heat-treated at higher temperatures. The fibers were significantly more difficult to process than the fibers; we were unsuccessful at fabricating good quality ESA coated fibers.

### *Polymer / Indicator-Salt Solution Cladding*

The need to find other substances which would adhere to the fiber and function as the cladding lead to the use of polytetrafluoroethane (PTFE). A known amount of CoCl<sub>2</sub> was dissolved in liquid PTFE and the solution was placed in a reservoir. The fiber core was drawn through the reservoir, depositing the cladding on the fiber. After an extended time in ambient conditions, the sensor was immersed in ethanol and any changes in spectra were observed.

Slight changes (on the order of several percent) in absorption of spectra were noted at approximately 685 nm in the PTFE-clad fibers, which is indicative of moisture changes in CoCl<sub>2</sub>. However, when the fiber was immersed in ethanol, the CoCl<sub>2</sub> washed away, which caused the few samples that were successfully fabricated to have unrepeatable results. The PTFE-clad fibers were extremely difficult to connectorize due to the brittle nature of the silica core, causing low yield of good quality sensors from the PTFE-clad fibers. The fibers also required long path lengths to sense humidity changes, and the hydrochromatic salts showed very low solubility in the PTFE. We concluded that we required higher sensitivity than the PTFE-clad fiber could provide.

Although the initial intent was to create an evanescent sensor, it was determined that the reflective sensor was better suited to the present applications. CRG utilized two materials to create reflective mode fiber sensors: sol-gel glass and doped ceramics.

### *Sol-Gel Glass*

Sol-gel glass was fabricated using the same process described in the Sol-Gel Cladding section, except that the sol was cast into molds before gelation. A variety of mold configurations were utilized.

We successfully created small beads of sol-gel glass. The resulting sol-gel glass was extremely sensitive to changes in humidity. The glass underwent a color change from a deep blue at low humidity,

### *Sol-Gel Glass*

Sol-gel glass was fabricated using the same process described in the Sol-Gel Cladding section, except that the sol was cast into molds before gelation. A variety of mold configurations were utilized.

We successfully created small beads of sol-gel glass. The resulting sol-gel glass was extremely sensitive to changes in humidity. The glass underwent a color change from a deep blue at low humidity, to a bright pink at ambient conditions. Though the sensitivity of the glass was high, the glass was extremely fragile, which is the same problem we experienced with the sol-gel films on glass. We concluded that we needed a material that exhibited high sensitivity, but packaged in a more durable substrate.

### *Doped Ceramics*

We had the most success with ceramics doped with  $\text{CoCl}_2$  or  $\text{CuCl}_2$ . Thin wafers of ceramic were soaked in indicator-salt / alcohol solutions, then dried.

The doped ceramic sensors demonstrated good sensitivity in a durable substrate. The changes in relative intensity were significant. Data was recorded at every one-percent change in relative humidity, as indicated by the hygrometer. Intensity peaks of up to 17% were observed for  $\text{CoCl}_2$  sensors, as shown in Figure 18, and greater than 10% for  $\text{CuCl}_2$ , as shown in Figure 19. (It should be noted that the data shown in the figure is indicative of relative humidity steps of 3-4%).

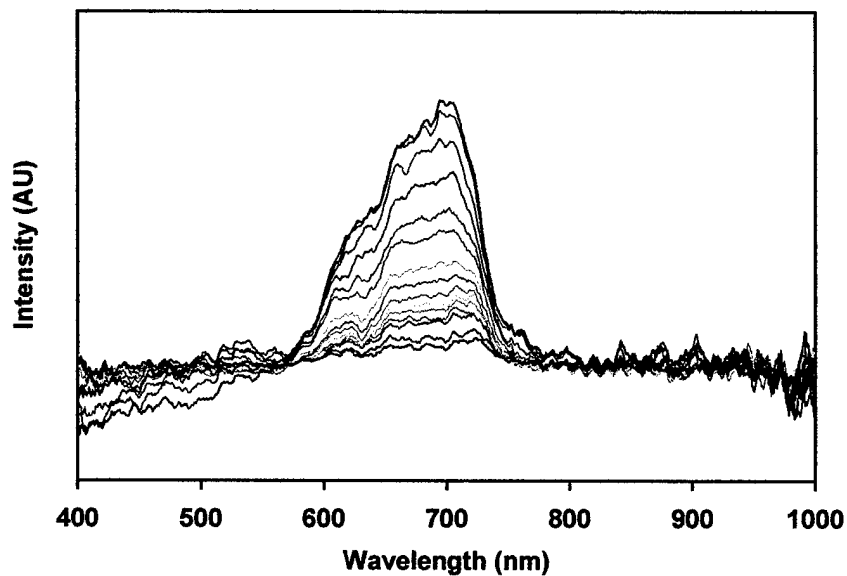


**Figure 18: Humidity Absorbance Spectrum for  $\text{CoCl}_2$  doped Ceramic Reflective Sensor**

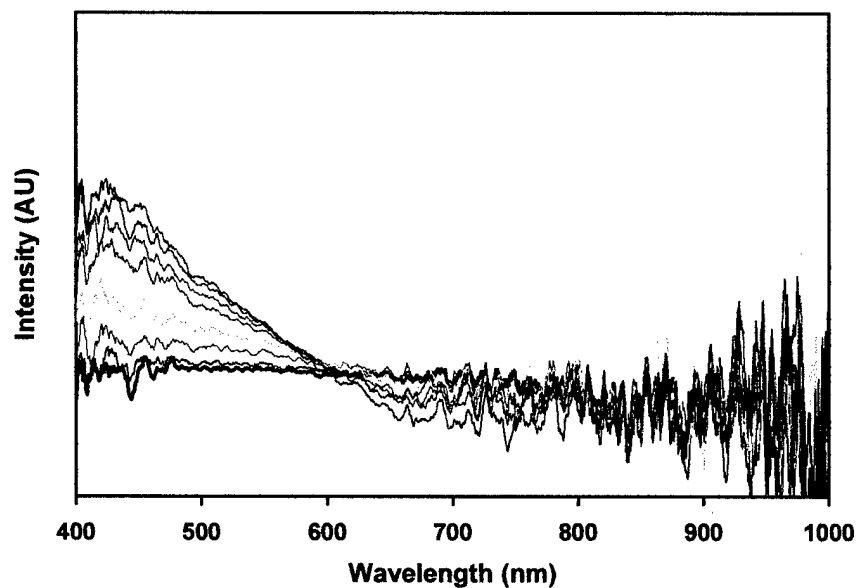


**Figure 19: Humidity Absorbance Spectrum for  $\text{CuCl}_2$  doped Ceramic Reflective Sensor**

Wavelength to wavelength ratios were taken to normalize the changes in intensity of the spectra. The nearly linear results shown in Figures 20 and 21 were indicative of a constant change in intensity of the spectra. For every one percent change in relative humidity, there was an approximate one percent change in intensity.

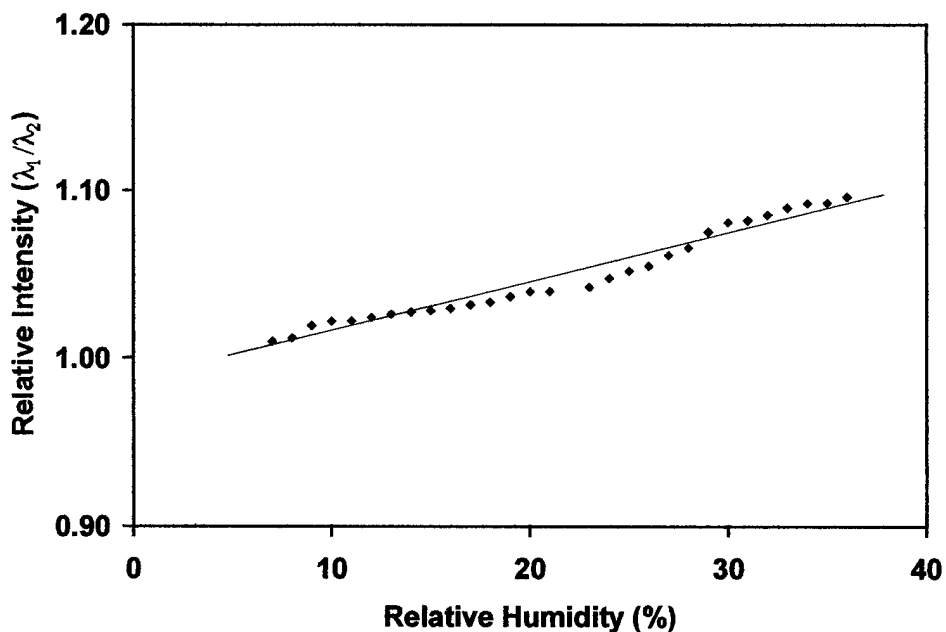


**Figure 20: Calibration Curves for Relative Humidity for  $\text{CoCl}_2$  doped Ceramic Reflective Sensor**

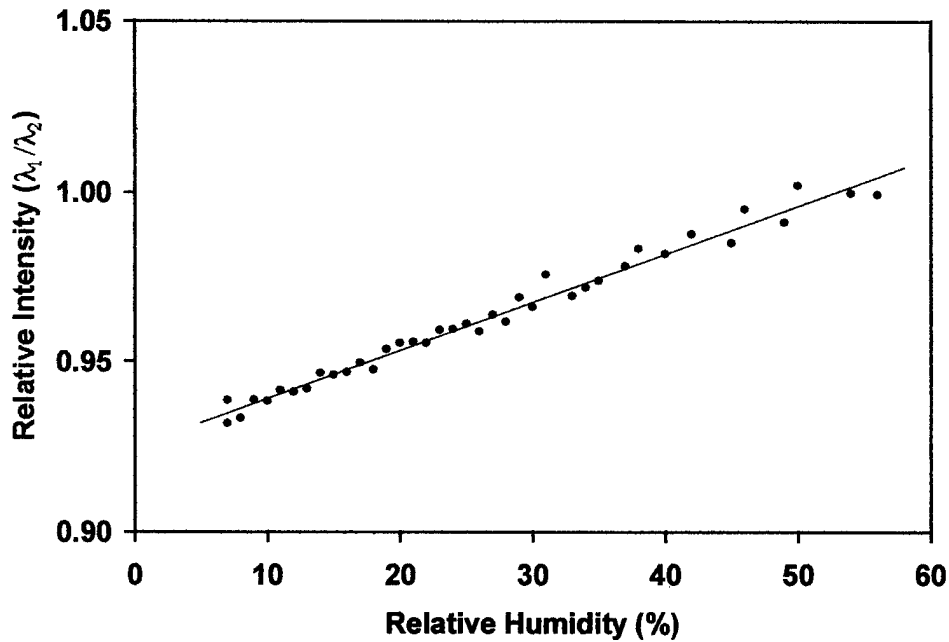


**Figure 21: Calibration Curves for Relative Humidity for CuCl<sub>2</sub> doped Ceramic Reflective Sensor**

Figure 22 shows the experimental setup for testing the reflective sensors. Sensors were subjected to decreasing- increasing- decreasing relative humidity cycles. These tests were performed multiple times. Repeatability and reproducibility was observed from each sample, and from sample to sample. Data was not collected for each run, due to the time required for acquisition and analysis, and therefore no error can be calculated.

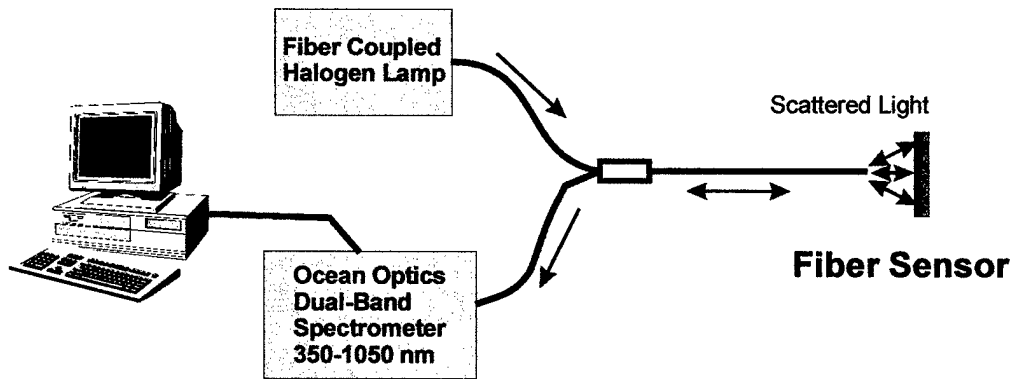


**Figure 22: Experimental Configuration and Approach**

## Conclusions

In this Phase I research program we successfully synthesized a high performance liquid crystal monomer and evaluated it for use as an adhesive. Experiments demonstrated the ability to thermally cure liquid crystalline monomer at temperatures below 150°C. This is important in reducing the cost and complexity of processing adhesively bonded joints. This material is also suitable for many elevated temperature applications based on the thermal stability data that showed the adhesive to be thermally stable to temperatures in excess of 300°C.

A fiber optic moisture sensor was also demonstrated in this program. Several approaches were investigated to fabricate a highly sensitive device capable of being integrated into the joint area. A doped ceramic approach was found to be the simplest and yielded the best sensitivity results.

Following discussions with the technical monitor and after evaluating the effort needed to develop either the material or the sensor, Cornerstone Research Group and the University of Dayton decided to focus the Phase II effort on further developing and characterizing the liquid crystal monomer. This research program will also investigate various processing parameters and methodologies. The monomer being developed is dual curing using either a thermal process or an e-beam exposure. Because the LC phase allows tight packing of molecules, it has a higher density than the isotropic phase. Cure in the smectic phase should result in lower overall cure shrinkage than typical isotropic monomers exhibit. Lower thermal expansion coefficients can also result from cure of a LC material. These materials characteristics should result in a high performance joining technology.

## References

- <sup>1</sup> J. Schultz, R. Chartoff, J. Ullett "Photopolymerization of Nematic Liquid Crystal Monomers for Structural Applications: Linear Viscoelastic Behavior and Cure Effects," *J. Polym. Sci.:Part B, Polym. Phys*, **36**, 1081-1089 (1998).
- <sup>2</sup> J. Schultz, R. Chartoff, J. Ullett "Photopolymerization of Nematic Liquid Crystal Monomers for Structural Applications: Linear Viscoelastic Behavior and Cure Effects," *J. Polym. Sci.:Part B, Polym. Phys*, **36**, 1081-1089 (1998).
- <sup>3</sup> J. Ullett, J. Schultz, T. Benson-Tolle, and R. Chartoff, "Thermal-Mechanical and Fracture Toughness Properties of Parts Made from Liquid Crystal Stereolithography Resins," *Proc. of the Solid Freeform Fabrication Symposium*, Austin, TX, 519-528 (1998).
- <sup>4</sup> D. Frich and J. Economy, "Thermally stable liquid crystalline thermosets based on aromatic copolyesters: preparation and properties," *J. of Poly. Sci. Part A. - Polymer Chemistry* v. 35, 1061-1067, (1997).
- <sup>5</sup> D. Frich and J. Economy, "Thermally stable liquid crystalline thermosets based on aromatic copolyesters: preparation and properties," *J. of Poly. Sci. Part A. - Polymer Chemistry* v. 35, 1061-1067, (1997).
- <sup>6</sup> Jones, Jr., R. E., Earls, J. D., and Hefner, Jr., R. E., "Process for Comparing Composites Based on Oriented Mesogenic Thermoset Resins," United States Patent 5,248,360, issued September 28, 1993.
- <sup>7</sup> J.W. Schultz, R.P. Chartoff, "Photopolymerization of Nematic Liquid Crystal Monomers for Structural Applications: Molecular Order and Orientation Dynamics," (in press) *Polymer* (1998).
- <sup>8</sup> R. P. Chartoff, J. S. Ullett, and D. A. Klosterman, "Advanced Materials Processing by Rapid Prototyping Methods," *Prototyping Technology International '97*, UK & International Press, 1997.
- <sup>9</sup> J.W. Schultz, R.T. Pogue, J.S. Ullett, and R.P. Chartoff, "Birefringence Thermal Analysis of Liquid Crystalline Monomers and Their Photopolymers," *J. Thermal Analysis*, vol. 49, 155-160, 1997.
- <sup>10</sup> J.W. Schultz, R.P. Chartoff, J.S. Ullett, "Photopolymerization of Nematic Liquid Crystal Monomers for Structural Applications: Linear Viscoelastic Behavior and Cure Effects," (in press) *Journal of Polymer Science: Part B: Polymer Physics*, (1998)
- <sup>11</sup> J.C. Bhatt, M.H. Dotrong, R.T. Pogue, J.S. Ullett, R.P. Chartoff, M.H. Litt, and X.T. Bi, "Synthesis and Photopolymerization of Liquid Crystalline Diacrylate Resins," *Polymer Preprints*, vol.38 no.1, 147-148, 1997.
- <sup>12</sup> J.C. Bhatt, M.H. Dotrong, R.T. Pogue, J.S. Ullett, and R.P. Chartoff, "Synthesis and Photocuring of Acetylene-Containing Diacrylate Monomers," *Polymer Preprints*, vol.38 no.1, 149-150, 1997.
- <sup>13</sup> J.W. Schultz, R.P. Chartoff, "Liquid Crystal Network Polymers from Oriented Monomers: Measurement of Molecular Order and Orientation Dynamics with Dielectric Analysis," *NATAS Notes*, vol.29 no.3, 20-25, 1997.
- <sup>14</sup> J. W. Schultz, J. S. Ullett, and R. P. Chartoff, "Novel Liquid Crystal Resins for Stereolithography - Mechanical Properties," *Proceedings of the 8th Solid Freeform Fabrication Symposium*, August 11 - 13, 1997, Austin, Texas.
- <sup>15</sup> R. T. Pogue, and R. P. Chartoff, "Novel Liquid Crystal Monomers for Stereolithography: Reaction Rates and Photopolymerization Conversion," *Proceedings of the 8th Solid Freeform Fabrication Symposium*, August 11 - 13, 1997, Austin, Texas.
- <sup>16</sup> J.S. Ullett, J.W. Schultz, and R.P. Chartoff, "Advanced High Temperature Resins for Stereolithography," *Proceedings of the Seventh International Conference on Rapid Prototyping* March 31 - April 3, 1997, San Francisco, CA, p. 203.
- <sup>17</sup> J. S. Ullett, J. W. Schultz, and R. P. Chartoff, "Novel Liquid Crystal Resins for Stereolithography - Processing Parameters," *Proceeding of the 6th European Conference on Rapid Prototyping and Manufacturing*, July 1- 3, 1997, Nottingham, England.
- <sup>18</sup> W. J. Bailey, "Cationic Polymerization with Expansion in Volume," *J. Macromol. Sci.-Chem.*, **A9(5)**, 849-865 (1975).
- <sup>19</sup> J. S. Ullett, S. J. Rodrigues and R. P. Chartoff, "Linear Shrinkage of Stereolithography Resins," *The Sixth Int. Conf. on Rapid Prototyping*, Dayton, OH., June 4-7, 1995.
- <sup>20</sup> J. S. Ullett, R. P. Chartoff, A. J. Lightman, J. P. Murphy, and J. Li, "Reducing Warpage in Stereolithography Through Novel Draw Styles," *The Fifth Int. Conf. on Rapid Prototyping*, Dayton, OH, June 12 - 15, 1994.
- <sup>21</sup> G. D. Davis, P. L. Whisnant and J. P. Wolff, Jr., "Monitoring Adhesive Bond Integrity with Electrochemical Impedance Spectroscopy," *Proceedings of the 41<sup>st</sup> International SAMPE Symposium*, 544-552, (1996).
- <sup>22</sup> Ding, J.Y., Shahriari, M.R., Sigel, Jr., G.H. "Fiber-Optic Moisture Sensors for High Temperatures," *Ceramic Bulletin*, 1991, **70**: 9, pp. 1513-1517.
- <sup>23</sup> Zhou, Q., Shahriari, M.R., Kritz, D., Sigel, Jr., G.H. "Porous Fiber-Optic Sensor for High-Sensitivity Humidity Measurements," *Analytical Chemistry*, 1988, **60**:20, pp. 2317-2320.
- <sup>24</sup> V. Ruddy, "Nonlinearity of absorbance with sample concentration and path length in evanescent wave spectroscopy using optical fiber sensors," *Opt. Engin.* vol. 33 no. 12, 3891-3894 (December 1994).
- <sup>25</sup> Hench, L.L., West, J.K. "The Sol-Gel Process," *Chemical Reviews*, **90**:1, pp.33-72, 1990.
- <sup>26</sup> Rosidian, A., Liu, Y., Claus, R.O. "Ionic Self-Assembly of Ultrahard ZrO<sub>2</sub>/Polymer Nanocomposite Thin-Films," accepted for publication in *Advanced Materials* in April 1998.